Journal of New Technology and Materials (JNTM)
J. New Technol. Mater.
Vol. 08, N°01 (2018)120-125

OEB Univ. Publish. Co.

1-formyl-3-phenyl-5-aryl-2-pyrazoline derivatives as corrosion inhibitors of steel in acidic medium: Computational simulations study.

I. Selatnia[a,b] and A. Sid[a,b*]

[a] *Laboratory of Applied Chemistry and Material Technology (LCATM). Material Sciences Departement. Larbi Ben M'Hidi University. Oum El Bouaghi. 04000. Algeria.*
[b] *Laboratory of Analytical Sciences, Materials and Environmental (LSAME). Material Sciences Department. Larbi Ben M'Hidi University. Oum El Bouaghi. 04000. Algeria.*

Corresponding author, email: madamesid9@yahoo.fr

Received date: Jan. 15, 2018; revised date: June 07, 2018; accepted date: June 08, 2018

Abstract

In this paper, inhibition reactivity of two synthesized pyrazoline derivatives namely: 1-Formyl-3-phenyl-5-(4-methylphenyl)-2-pyrazoline (P1) and 1-Formyl-3-phenyl- 5-(4-chlorophenyl) -2-pyrazoline (P2), towards steel corrosion was studied by using quantum chemical calculations and molecular dynamics simulation (MD) to give more insights into the action mode of studied inhibitors. Several parameters such as E_{HOMO}, E_{LUMO}, energy gap (ΔE), fraction of electron transfers (ΔN) and Fukui index have been studied. Moreover, MD simulation is performed to simulate the best adsorption configuration of the investigated inhibitors on Fe (1 1 0) surface. Results indicate that the active sites of the molecules were mainly located on the pyarazoline ring and on the carbonyl group. The binding strength of the studied inhibitor molecules on Fe surface follows the order P1>P2.

Keywords: Corrosion inhibitors; Molecular dynamics simulation; pyrazoline derivatives.

1. Introduction

Corrosion of metals is considered as a major problem in many sector of industries, which caused a huge damaged of materials and financial pert. To provide this problem several methods were employed but the use of corrosion inhibitor is one of the most practical and effective method for protection of metals [1]. In recent years, organic compounds especially N-heterocyclic compounds have been used as an effective corrosion inhibitor [2-4]. Pyrazoline derivatives are the most important heterocyclic compounds due to their significant antimicrobial properties [5], antifungal [6], antidepressant [7], and anti- inflammatory [8]. Recently, these compounds are reported as a good corrosion inhibitor of steel in acidic medium [9-10]. Several experimental techniques have been utilized to evaluate the inhibition efficiency of an inhibitor but they are expensive and time-consuming; also, it is deficient to explain the inhibition mechanism [11-12]. Actually, and with the development of computer simulation techniques, the use of quantum chemical methods in corrosion inhibitor studies draws much attention. Quantum chemical calculations and Molecular dynamics simulation (MD) become fast, inexpensive and effective tools to determine the molecular structure, elucidate the electronic structure and reactivity as well as predict the corrosion inhibition performance of organic compounds [13-15]. The aim of this study is a prediction of the corrosion efficiency and inhibition mechanism of two pyrazoline derivatives synthesized and published in our previous work [16], namely 1-Formyl-3-phenyl -5- (4-methylphenyl)-2-pyrazoline (P1) and 1-Formyl-3- phenyl-5-(4-chlorophenyl)-2-pyrazoline (P2) (see Fig.1) . These techniques approach have been performed to determine the most effective corrosion inhibitor among them theoretically.

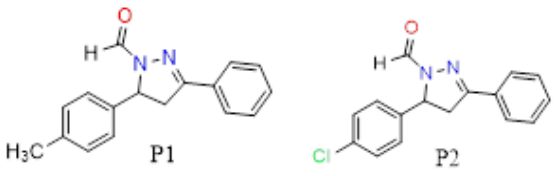

Figure 1. Chemical structures of studied molecules.

2. Computational details

2.1. Quantum chemical calculation

Quantum chemical calculations were performed on the pyrazoline derivatives using DMol[3] module of materials studio software [17]. Different parameters were calculated using double numerical polarization (DNP) basis set in conjunction with generalized gradient approximation (GGA) functional of Becke exchange plus Lee–Yang–Parr

correlation (BLYP) [18]. The COSMO model has been included to study the effect of solvent aqueous solution.

2.2. Molecular dynamics (MD) simulation

Molecular dynamics simulation of the two-pyrazoline derivatives were carried out in a simulation box (24.82×24.82×35.63 A°) with periodic boundary conditions using Discover module in Materials studio 7.0. More simulation details may found elsewhere [19-21]. The simulation was performed at 298 K, NVT ensemble, with time step of 1 fs and simulation time of 50 ps using the COMPASS force field [22]. The interactions between the inhibitor and Fe (110) can be established by interaction and binding energies calculated using the following equations [23]:

$$E_{interaction} = E_{total} - \left(E_{surface\ +H_2O} + E_{inhibitor}\right) \quad (1)$$

$$E_{binding} = -E_{interaction} \quad (2)$$

Where the E_{total} is defined as the total energy of the entire system, $E_{surface\ +H_2O}$ is defined as the total energy of Fe (110) surface and solution without the inhibitor and the $E_{inhibitor}$ is the energy of the adsorbed inhibitor molecule on the surface.

3. Results

3.1. Quantum chemical calculation

3.1.1. Equilibrium structure geometry

The optimized geometries of molecules P1 and P2 are represented in Fig. 2, and their calculated parameters such as the bond lengths and bond angles are summarized in Table 1. The inspection of Table 1 shows that all bond lengths and angles in the pyrazoline ring are within the expected range and there is a little difference between their values in the two tested compounds. The C=N and C-N bond lengths of the pyrazoline ring of P1 and P2 compounds are found to range within 1.283-1.285 A° and 1.508-1.514 A° respectively, similarly to those found in analogous structures (C=N: 1.291-1.300 A°) and (C-N: 1.482- 1.515 A°) [24, 25]. Therefore, the N10-N11 bond length of P1 and P2 is 1.403 and 1.402 A°, respectively, which is close to the mentioned data (1.373-1.380) [26]. The observed difference could be attributed to the effect of the substitution of carbonyl group and phenyl rings on the pyrazoline ring [27]. From the above-mentioned bond lengths of the optimized P1 and P2 compounds, we can conclude that their geometry configuration is ideal [25].

Table 1. Bond length (A°), bond angle (°) for the optimized molecules P1 and P2

Geometry parameters	P1	P2
Bond length		
C7-C8	1.534	1.535
C8-C9	1.504	1.500
C9-N10	1.285	1.283
N10-N11	1.403	1.402
N11-C7	1.514	1.508
N11-C20	1.358	1.360
C20-O21	1.238	1.234
Bond angle		
C7-C8-C9	103.297	103.637
C8-C9-N10	114.695	114.252
C9-N10-N11	108.431	108.035
N10-N11-C7	112.165	112.047
N11-C7-C8	100.795	100.652
N11-C20-O21	126.010	125.246

3.1.2. Frontier orbital energies

In general, the predicting of the adsorption sites and/or fragments and the molecular reactivity of inhibitors are related to frontier molecular orbital (FMOs) involving the highest occupied and lowest unoccupied molecular orbital energies, (E_{HOMO}) and (E_{LUMO}), respectively. The E_{HOMO} energy is often associated with the electron donating ability of a molecule; therefore, E_{LUMO} depends upon the tendency of a molecule to accept electrons. It was generally established that the inhibition efficiency increases with the enhancement of E_{HOMO} values. The higher is the value of E_{HOMO} of an inhibitor, the greater is its ability of donating electrons to unoccupied d-orbital of the metal atoms [28]. Additionally, the energy gap ΔE between HOMO and LUMO levels of the molecule ($\Delta E = E_{HOMO} - E_{LUMO}$) is an important index, since the ΔE value decreases when the reactivity of an inhibitor increases, and hence increases its adsorption ability [27]. The spatial distribution of the frontier molecular orbital's HOMO and LUMO of the studied inhibitors are represented in Fig 2, and there quantum chemical parameters are listed in Table 2.

Fig. 2 shows that the electron density distribution of HOMO and LUMO is almost similar and strongly spread on the pyrazoline ring, carbonyl group and phenyl ring. This kind of distribution could be attributed to the presence of conjugation effect and high electron density of these segments, reflecting their involvement in the adsorption process on the metal surface. [27].

From Table 2, it can be seen that P1 has a higher E_{HOMO} and a lower ΔE value than P2 , which indicates that P1 has more ability to donate the electrons to unoccupied *d*-orbital of the metal. Whereas, the E_{LUMO} of P2 is lower than P1, which could be attributed to the presence of –Cl group

in the phenyl ring. This result is often interpreted by the presence of complicated interactions perhaps playing the crucial role in the adsorption process [29].

Table 2. Quantum chemical parameters of the studied compounds

	P1	P2
HOMO	-5.423	-5.647
LUMO	-2.143	-2.363
ΔE	3.280	3.284
I	5.423	5.647
A	2.143	2.363
χ	3.783	4.005
γ	1.640	1.642
ΔN	0.316	0.248

The ionization potential (I) and electron affinity (A) are related to the HOMO and LUMO energies, respectively, as follows [29]:

$I = -E_{HOMO}$ (3)

$A = -E_{LUMO}$ (4)

The absolute electronegativity (χ) and global hardness (γ) can be calculated by using the following equations [30]:

$$\chi = (I + A)/2 \quad (5)$$

$$\gamma = (I - A)/2 \quad (6)$$

The fraction of electron (ΔN) transferred is calculated using the following equation [30]:

$$\Delta N = \frac{\chi_{Fe} - \chi_{inh}}{2(\gamma_{Fe} + \gamma_{inh})} \quad (7)$$

Where the theoretical values of χ_{Fe} and γ_{Fe} are 7.0 eV and 0 eV, respectively, Recently, it was reported that the value of χFe = 7 eV is not acceptable theoretically since electron-electron interactions were not considered, only free electron gas Fermi energy of iron was considered [29]. Therefore, the researchers are recently using work function (ϕ) of the metal surface instead of χ_{Fe}, and the equation (7) is rewritten as follow:

$$\Delta N = \frac{\phi - \chi_{inh}}{2(\gamma_{Fe} + \gamma_{inh})} \quad (8)$$

The obtained DFT derived ϕ for Fe (110) surface "the higher stabilization energy" is 4.82 eV [31].

I. Lukovit has reported that the inhibition efficiency increased with increasing electron donating ability at the metal surface when the value of ΔN<3.6 [32]. In the present study, we observed (via Table 2) that the calculated values ΔN of both P1 and P2 are positive and lower than 3.6, implying the high ability of these molecules to donate electrons to the iron surface.

It is concluded from the discussion above that the inhibition efficiency of this inhibitors follows the order: P1>P2.

3.1.3. Local reactivity

The local reactivity of the inhibitors was analyzed by means of Fukui function(f_k) which is defined as the first derivative of the electronic density ($\rho(\vec{r})$)with respect to the number of electrons N in a constant external potential $v(\vec{r})$ [33]:

$$f_k = \left(\frac{\partial \rho(\vec{r})}{\partial N}\right)_{v(\vec{r})} \quad (9)$$

The condensed Fukui function can be calculated as follows:

$$f_k^+ = q_k(N+1) - q_k(N) \quad (10)$$

$$f_k^- = q_k(N) - q_k(N-1) \quad (11)$$

Where $q_k(N+1), q_k(N)$ and $q_k(N-1)$are the atomic charges of the anionic, neutral and cationic species, respectively.

An analysis of the Fukui indices for nucleophilic and electrophilic sites are represented in Tables 3. The nucleophilic and electrophilic attacks are respectively characterized by f_k^+ andf_k^-.

In P1, atoms C9, N11, C12, O21 and in P2, atoms C9, N10, N11, and O21 are the most susceptible sites for nucleophilic attacks. On the other hand, atoms N10, C15, C17, C20 in P1 and atoms C9, N10, C15 in P2 are the most probable centers for electrophilic attacks. Nevertheless, in P1, the atom C9 has the highest value of f_k^- whereas in P2, the atom O21 has the highest value of f_k^- .These sites are the most reactive for nucleophilic attacks. As for $f_k^{\mp}$, electrophilic attacks, N10 has the highest value for both P1 and P2.

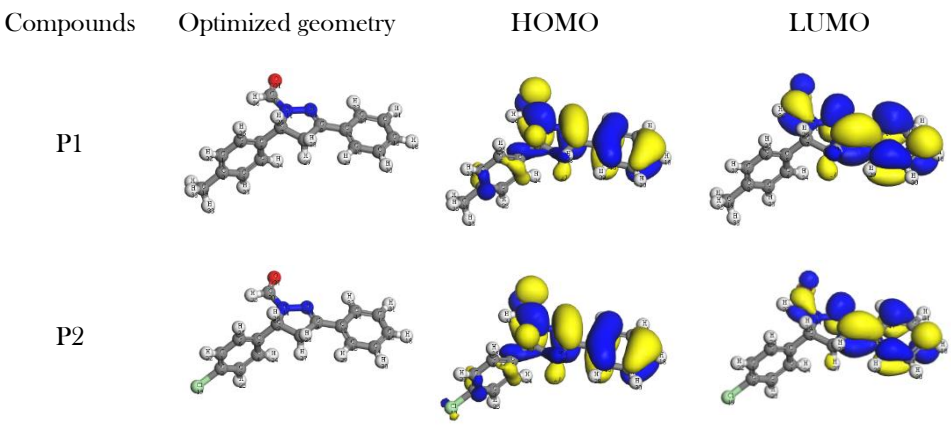

Figure 2. The Optimized geometry and distribution of HOMO and LUMO of P1 and P2 molecules.

Table 3. The calculated Fukui function of the P1 and P2 molecules

	P1		P2	
Atoms	f_k^-	f_k^+	f_k^-	f_k^+
C(1)	0.071	-0.060	0.014	-0.003
C(2)	-0.029	0.056	0.006	0.014
C(3)	0.037	-0.027	0.004	0.007
C(4)	0.064	-0.044	0.018	0.000
C(5)	-0.022	-0.012	0.003	-0.041
C(6)	-0.041	0.068	0.009	0.019
C(7)	0.016	-0.035	-0.034	0.017
C(8)	-0.050	-0.004	-0.033	-0.023
C(9)	**0.154**	0.040	**0.098**	**0.113**
N(10)	0.037	**0.192**	0.081	**0.137**
N(11)	**0.077**	-0.013	**0.092**	-0.029
C(12)	**0.082**	-0.057	0.016	0.016
C(13)	0.073	0.028	0.046	0.063
C(14)	0.007	0.014	0.015	0.010
C(15)	0.042	**0.138**	0.083	**0.116**
C(16)	0.008	-0.005	0.004	-0.002
C(17)	-0.039	**0.158**	0.041	0.087
C(19)	0.004	-0.013	-	-
Cl(19)	-	-	0.024	0.008
C(20)	0.028	**0.113**	0.030	0.064
O(21)	**0.145**	0.047	**0.122**	0.063

3.2. Molecular dynamics simulation

Nowadays many studies dealing with corrosion inhibition use the molecular dynamics simulation as an important tool in understanding the interaction between inhibitors and metal surface.

Fig.3 represents the energy and temperature equilibrium curves obtained using MD simulation for both P1 and P2 molecules. As can be seen, both energy and temperature reach balance, indicating that, the whole system have reached equilibrium [34]. The equilibrium adsorption configuration of the studied inhibitor on Fe (1 1 0) surface is illustrated in Fig. 4 and the calculated interaction energy and binding energy are listed is Table 4. It could be observed from Fig.4, that the studied inhibitor molecules are adsorbed close to the Fe surface. The high negative values of the binding energies (via Table 4) indicate that the adsorption of inhibitors on Fe (1 1 0) surface is spontaneous, strong, and stable [28]. The binding energies are found to increase in the order P1 > P2, showing that P1 adsorbs more strongly on the iron surface and possesses better inhibition performance than P2. This result is in a good agreement with the quantum chemistry analysis mentioned above.

Table 4. Interaction energies between the inhibitors and Fe (110) surface in aqueous phase (kJ/mol).

System	Binding energy	Interaction energy
Fe+P1	635.952	-635.952
Fe+P2	618.076	-618.076

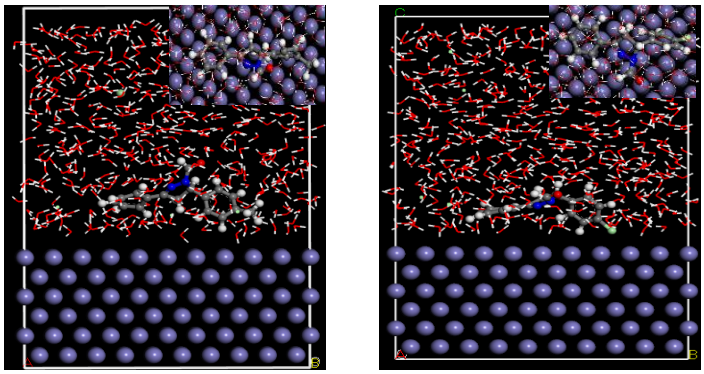

P1 P2

Figure 4. Equilibrium adsorption configurations of the studied inhibitors on Fe (1 1 0) surface in water solution (top and side view)

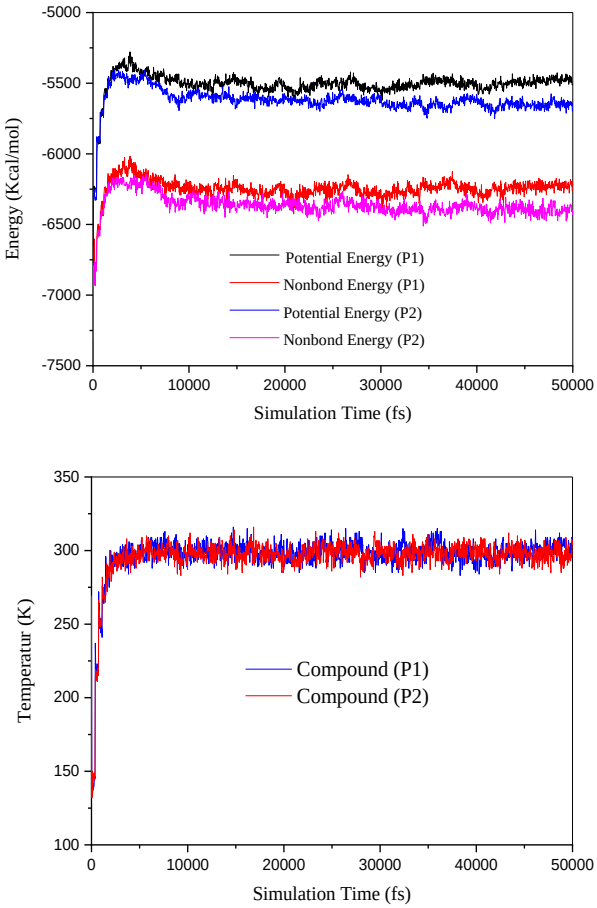

Figure 3. Energy and temperature equilibrium curves obtained using MD simulation for P1 and P2 molecules.

4. Conclusion

Quantum chemical calculations and Molecular dynamics simulation (MD) were employed to predict the inhibition efficiencies of two pyrazoline derivatives as corrosion inhibitors for carbon steel. The following insightful conclusions can be obtained from this present study:

- Inhibition efficiency was enhanced with an increase in E_{HOMO}. P1 had the highest inhibition efficiency because it had the highest HOMO energy and ΔN values, and it was most capable of offering electrons.
- The distribution of electronic density and fukui analysis showed that the pyrazoline derivatives compounds had many active electron-donating centers.
- MD simulation indicate that all values of binding energy are negative and following the order: P1>P2, which is in accordance with the result obtained from quantum chemical calculations.
- This study has shown that theoretical calculations and MD simulation can be used as reliable approaches to screen organic corrosion inhibitors prior to experimental validation.

5. References

[1] A. Ostovari, S. M. Hoseinieh, M. Peikari, S.R. Shadizadeh, S.J. Hashemi, Corros. Sci. 51 (2009) 1935.

[2] M. Bouklah, N. Benchat, B. Hammouti, A. Aouniti, S. Kertit, Mater. Lett. 60 (2006) 1901.

[3] M. Lebrini, F. Robert, H. Vezin, C. Roos. Corros. Sci. 52 (2010) 3367.
[4] N.O. Eddy, H. Momoh-Yahaya, E. E. Oguzie. RCS. Adv. 6 (2015) 203.
[5] K. Ramalingam, G. X. Thyvekikakath, K. D. Berlin, R. W. Chesnut, R. A. Brown, N. N. Durham, S. E. Ealick, D. VanDerHelm, J. Med. Chem. 20 (1977) 847.
[6] S. S. Korgaokar, P. H. Patel, M. J. Shah, H. H. Parekh, Indian J. Pharm.Sci. 58(1996) 222.
[7] P. Y. Rajendra, R. A.Lakshmana, L.Prasoona, K.Murali, K. P. Ravi, Bioorg. Med. Chem. Lett. 15 (2005) 5030.
[8] O. A. Fathalla, M. E. A.Zaki, S. A.Swelam, S. M. Nofal, W. I. El-Eraky, Acta Pol. Pharm. 60 (2003) 51.
[9] H. Ma, S. Chen, Z. Liu, Y. Sun, J. Mol. Struct. 774 (2006) 19.
[10] K. Cao, W. Li, L. Yu, Int. J. Electrochem. Sci. 7 (2012) 806.
[11] E. E. Ebenso, D. A. Isabirye, N. O. Eddy, Int. J. Mol. Sci. 11(2010) 2473.
[12] M. Bouayed, H. Rabaa, A. Srhiri, J. Y. Saillard, A. B. Bachir, A. L. Beuze, Corros. Sci. 41 (1998) 501.
[13] L. Guo, W.P. Dong, S.T. Zhang, RSC Adv. 4 (2014) 41956.
[14] W. Wang, Z. Li, Q. Sun, A. Du, Y. Li, J. Wang, S. Bi, P. Li, Corros. Sci. 61 (2012) 101.
[15] K. F. Khaled, Electrochim. Acta. 53 (2008) 3484.
[16] A. Sid, K. Lamara, M. Mokhtari, N.Ziani, P. Mosset, Eur. J. Chem. 2 (3) 2011 311.
[17] Materials Studio, Revision 7.0, Accelrys Inc., San Diego, USA, 2013.
[18] J.R. Mohallem, T.O. Coura, L.G. Diniz, G. Castro, D. Assafráo, T. Heine, J. Phys. Chem. A 112 (2008) 8896.
[19] V. Srivastava, J. Haque, C. Verma, P. Singh, H. Lgaz, R. Salghi, M.A. Quraishi, J. Mol. Liq, 244 (2017) 340.
[20]H. Lgaz, R. Salghi, K. S. Bhat, A. Chaouiki, Shubhalaxmi, S. Jodeh, J. Mol. Liq, 244 (2017) 154.
[21] B. Xu, W. Gong, K. Zhang, W. Yang, Y. Liu, X. Yin, H. Shi, Y. Chen, J. Taiwan. Inst. Chem. E. 51(2015) 193.
[22] H. Sun, J. Phys. Chem. B. 102 (1998) 7338.
[23] Z. Zhang, N.C. Tian, X.D. Huang, W. Shang, L. Wu, RSC Adv. 6 (2016) 22250.
[24] F. Jian a, P. Zhao, H. Guo, Y. Li, Spectrochim. Acta Part A 69 (2008) 647.
[25] A. Sid, A. Messai, C. Parlak, N. Kazanc, D. Luneau, G. Kesan, L. Rhyman, I. A. Alswaidan, P.Ramasami. J. Mol. Struct. 1121 (2016) 46.
[26] C.J. Fahrni, L.C. Yang, D.G. VanDerveer, J. Am. Chem. Soc. 125 (2003) 3799.
[27] G. Gece, Corros. Sci. 50 (2008) 2981.
[28] H. Mi, G. Xiao, X. Chen, Comput. Theor. Chem. 1072 (2015) 7.
[29] H. Lgaz, K. S. Bhat, R. Salghi, Shubhalaxmi, S. Jodeh, M. Algarra, B. Hammouti, I. H. Ali, A. Essamri. J. Mol. Liq, 238 (2017) 71.
[30] I.B. Obot, D.D. Macdonald, Z.M. Gasem, Corros. Sci. 99 (2015) 1.
[31] Z. Cao, Y. Tang, H. Cang, J. Xu, G. Lu, W. Jing, Corros. Sci. 83 (2014) 292.
[32] I. Lukovits, E. Kálmán, F. Zucchi, Corrosion. 57 (2001) 3.
[33] F. De Proft, J. M. L. Martin, P. Geerlings, Chem. Phys. Lett. 256 (1996) 400.
[34] J. Zeng, J. Zhang, X. Gong, J. Chem. Theory. Comput. 963 (2011) 110.